Electronic supplementary materials *Mendeleev Commun.* 2022, **32**, 374–376

Mechanism of hydride abstraction in the electrocyclic phototransformation of heterostilbene

Alina E. Saifutiarova, Yury V. Fedorov, Elena E. Gulakova and Olga A. Fedorova

Table of contents

Experimental Section

All solvents and other reagents are commercial products (Acros, Aldrich, Merck) and were used without further purification. Deionized water with resistivity ≥ 18 MΩ cm^{-1} was used for measurements.

Synthesis of E-1 was performed as described [S1]. A mixture of 3,4-dimethoxybenzaldehyde (300 mg, 1.80 mmol), 3-methylpyridazine (0.16 mL, 1.80 mmol) and potassium *tret*-butoxide (202 mg, 1.80 mmol) in abs. DMF (4 ml) was stirred at room temperature for 4 h. The mixture was diluted with water (2 ml) and concentrated *in vacuo*. The obtained solid was dissolved in water (30 ml) and extracted with dichloromethane (5×20 ml). The organic layers were combined, and the solvent was removed.

Quantum yield of reactive oxygen species (ROS) generation

The iodide method. Iodide reagent: a mixture of potassium dihydrogen phosphate (0.17 g), ammonium molybdate (0.05 mg), potassium iodide (0.49 g) and 1 M NaOH (0.21 ml) was diluted in distilled water (24.75 ml). An appropriate quantity of the tested compound was dissolved in the iodide reagent to reach the concentration of $8 \cdot 10^{-5}$-$1.42 \cdot 10^{-4}$. Then 2.5 ml of the resulting solution was put in a 1cm quartz cuvette and irradiated with light (λ_{ex}= 382 nm) within 10 minutes. The spectrum of the solution was measured immediately after the irradiation and the absorbance of triiodide at 351nm was recorded. For each measurement ca. 6 light doses were used to reach the absorbance of potassium triiodide about 0.1-0.5.

Singlet oxygen quantum yield of the studied samples was determined by the following equation [S2]:

$$\Phi = \Phi_R \cdot \frac{V \cdot (1 - 10^{-A_R})}{V_R \cdot (1 - 10^{-A})} \quad ,$$

where A_R - optical density of standard photosensitizer (eosin) solution at the excitation wavelength; A - optical density of investigated substance solution at the excitation wavelength; V/V_R is the tangent of the slope of the linear section of the graph of the dependence of the optical density of the trap (KI) on the exposure time; Φ_R is the singlet oxygen quantum yield of the standard photosensitizer in the solvent used for the experiment. According to the literature [S3] for eosin in water, the Φ_R value is 0.52.

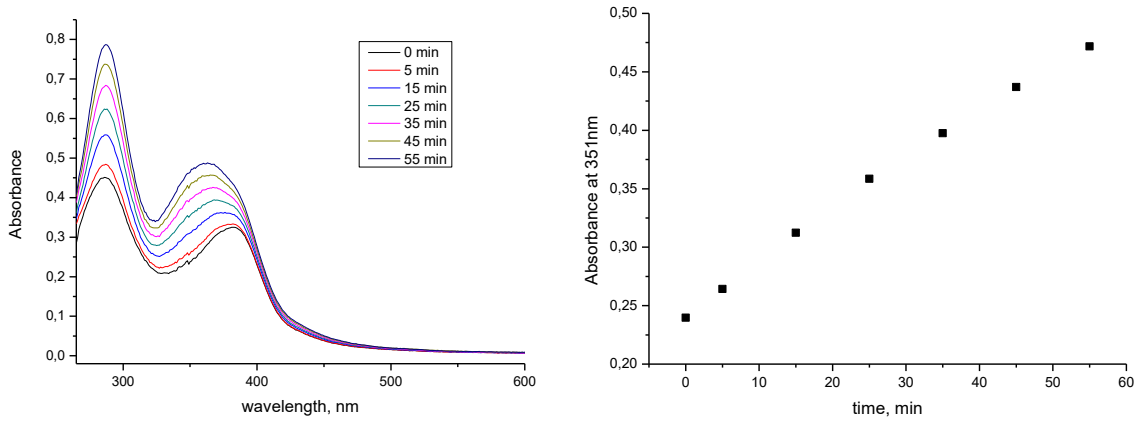

Figure S1 Spectral changes during the photolysis of a solution of compound **2** in KI (left) and the kinetics of KI_3 formation (right) at λ = 351 nm. $C_2 = 9 \cdot 10^{-5}$ M.

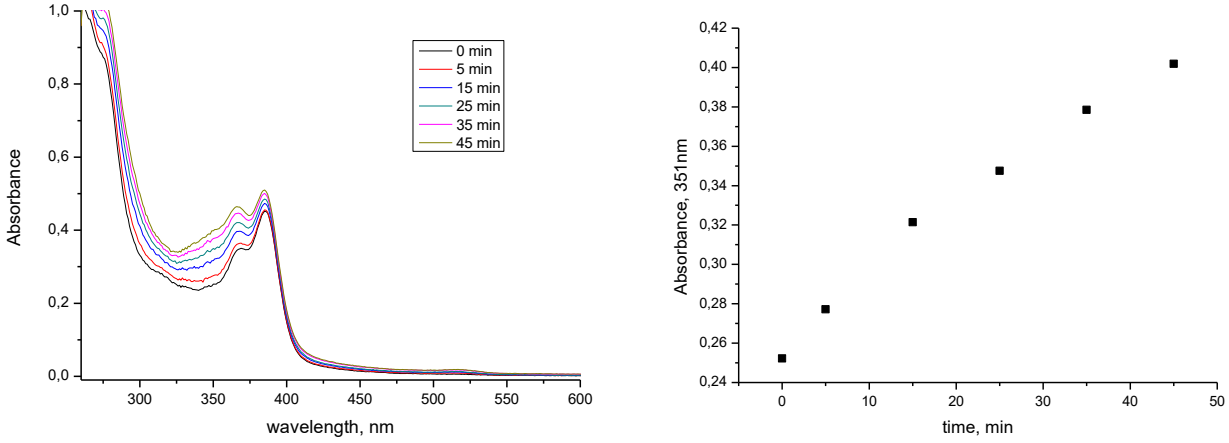

Figure S2 Spectral changes during the photolysis of a solution of compound **3** in KI (left) and the kinetics of KI_3 formation (right) at λ = 351 nm. $C_3 = 8 \cdot 10^{-5}$ M.

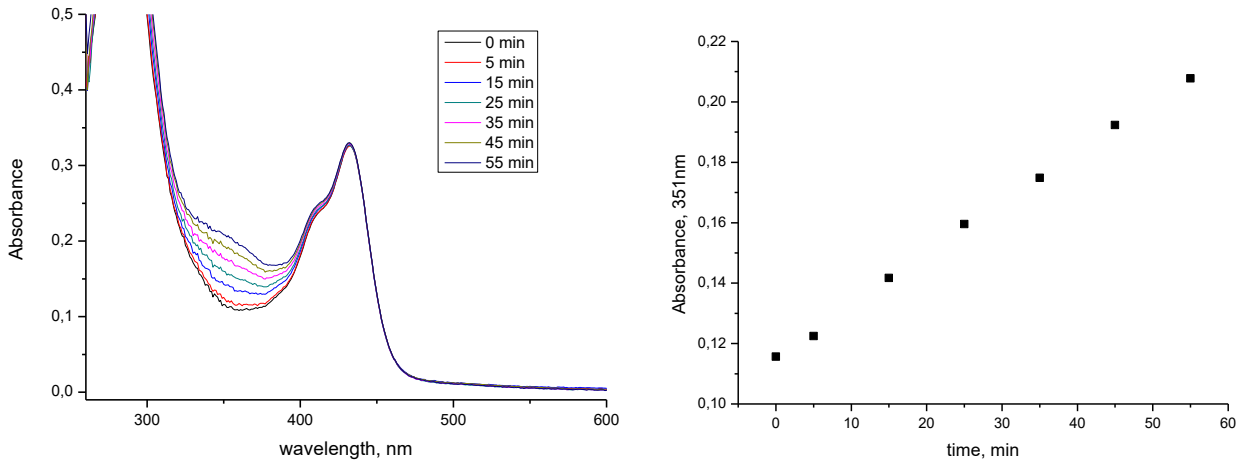

Figure S3 Spectral changes during the photolysis of a solution of compound **4** in KI (left) and the kinetics of KI_3 formation (right) at λ = 351 nm. $C_{\mathbf{4}} = 1.42 \cdot 10^{-4}$ M.

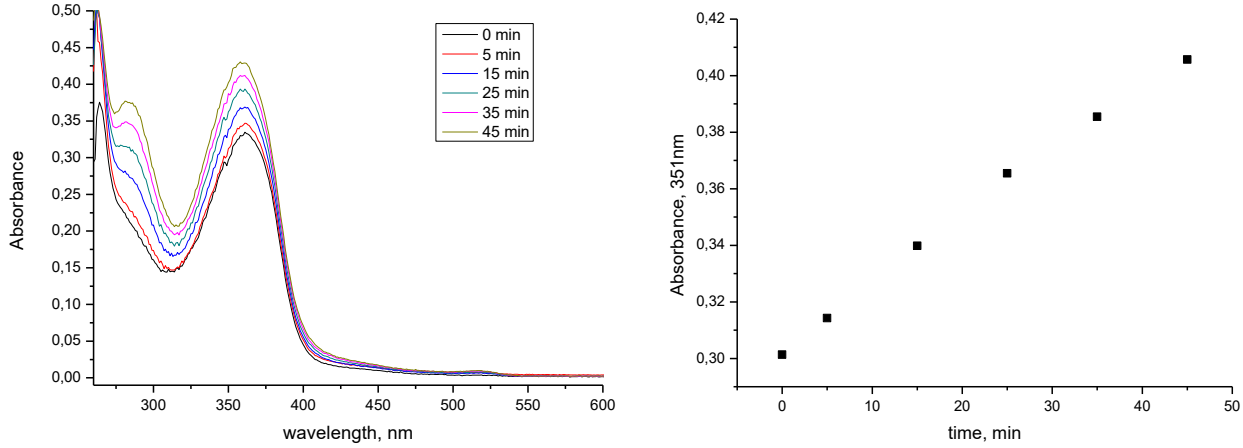

Figure S4 Spectral changes during the photolysis of a solution of compound **5** in KI (left) and the kinetics of KI_3 formation (right) at λ = 351 nm. $C_{\mathbf{5}} = 1 \cdot 10^{-4}$ M.

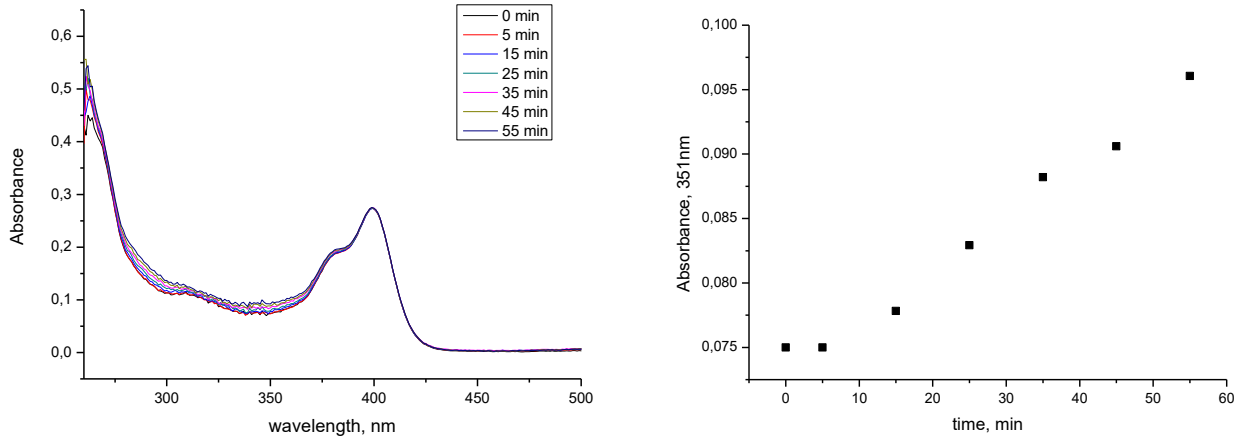

Figure S5 Spectral changes during the photolysis of a solution of compound **6** in KI (left) and the kinetics of KI_3 formation (right) at λ = 351 nm. $C_{\mathbf{6}} = 4 \cdot 10^{-5}$ M.

Steady-state optical measurements

The photochemical transformations were induced by irradiation of aqueous solutions of **1** with a high pressure mercury lamp (DRK-120, 120 W). The particular lines of the mercury lamp spectrum with λ = 313 and 365nm were isolated by glass filters from the standard set of colored optical glasses. The photo-processes were studied in a 10 mm quartz cell with stirring.

The self-developed program Sa3.3 (Simulation–adjustement) allowing the numerical simulation of the concentration of the various species versus time and the optimization of the parameter values until a good fit is obtained with selected experiments was used to analyze the three-species system [S4, S5].

The kinetic scheme characterizing the photochemical processes was as follows:

$$A \xrightarrow{hv1(phi0)} B$$
$$B \xrightarrow{hv1(phi1)} A$$
$$B \xrightarrow{hv1(phi2)} C$$

where A is *E*-**1**, B is *Z*-**1** and C is **2**.

The following parameters, variables, data and differential equations were used in the calculations in the Sa3.3 program:

Created parameters:
p[0]: phi0
p[1]: phi1
p[2]: phi2
p[3]: I1
p[4]: eps1.A
p[5]: eps1.B
p[6]: eps1.C
p[7]: eps2.A
p[8]: eps2.B
p[9]: eps2.C

Created variables:
ca[0][] <=> y[0]: A
ca[1][] <=> y[1]: B
ca[2][] <=> y[2]: C
ca[3][]: A1
ca[4][]: A2

Sa3.3_data:
A1 = y[0]*p[4] + y[1]*p[5] + y[2]*p[6];
F1 = p[3]*(1 - pow(10.0, -A1))/A1;
v0 = p[0]*F1*p[4]*y[0]; *// A ph1-> B*
v1 = p[1]*F1*p[5]*y[1]; *// B ph1-> A*
v2 = p[2]*F1*p[5]*y[1]; *// B ph1-> C*

Differential equations:
dy[0] = - v0 + v1; *// d[A]/dt*
dy[1] = v0 - v1 - v2; *// d[B]/dt*
dy[2] = v2; *// d[C]/dt*

where F1– the intensity of absorbed light (365 nm);
A1 – total absorbance at the irradiation wavelength (365 nm);
I1 – incident irradiation intensity at 365 nm;
Eps1.A, Eps1.B and Eps1.C – molar absorption coefficients of *E*-**1**, *Z*-**1** and **2**;
phi0, phi1 and phi2 – quantum yields of photoreactions **A→B**, **B→A** and **B→C**.

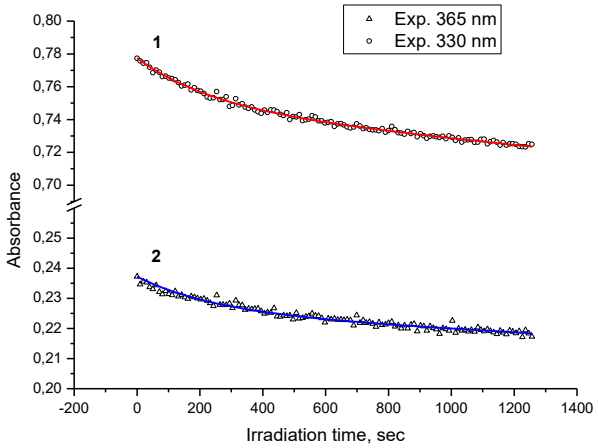

Figure S6 Changes in the absorption of $3 \cdot 10^{-5}$ M solution of **1** in H_2O at a wavelength of 330 nm (*1*) and 365 nm (*2*) depending on the time of irradiation with 365 nm light.
$I_0 = 3.8356 \cdot 10^{-6}$ Einstein dm^{-3} s^{-1}, optical path length: 10 mm.

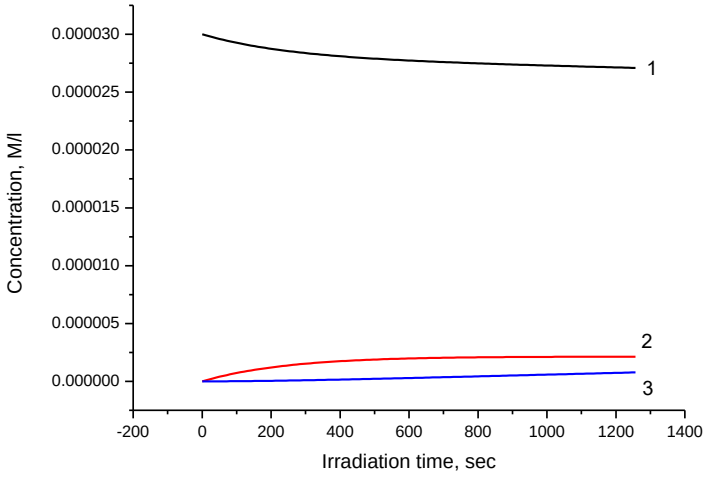

Figure S7 Changes in the concentrations of *E*-**1** (*1*), *Z*-**1** (*2*) and electrocyclic product **2** (*3*) upon irradiation of a $3 \cdot 10^{-5}$ M solution of trans-**1** in H_2O with 365 nm light.
$I_0 = 3.8356 \cdot 10^{-6}$ Einstein dm^{-3} s^{-1}.

UV-vis spectra were measured using a two channel spectrophotometer Varian-Cary 300. Fluorescence spectra were measured at 20±1 °C with a Cary Eclipse spectrofluorometer (Agilent).

All measured fluorescence spectra were corrected for the nonuniformity of detector spectral sensitivity. Coumarin 343 in ethanol (quantum yield of fluorescence φ^{fl} = 78.0%) [S4] was used as a reference for quantum yield measurements [S2]. The fluorescence quantum yields were calculated by eqn (1),

$$\varphi^{fl} = \varphi_R^{fl} \frac{S \cdot (1-10^{-A_R}) \cdot n^2}{S_R \cdot (1-10^{-A}) \cdot n_R^2} \quad , \qquad (1)$$

where φ^{fl} and $\varphi^{fl}{}_R$ are the fluorescence quantum yields of the studied solution and the standard compound, respectively; A and A_R are the absorption of the studied solution and the standard respectively; S and S_R are the areas underneath the curves of the fluorescence spectra of the studied solution and the standard respectively; and n and n_R are the refraction indices of the solvents for the substance under study and the standard compound. The quantum yields were calculated using corrected fluorescence spectra.

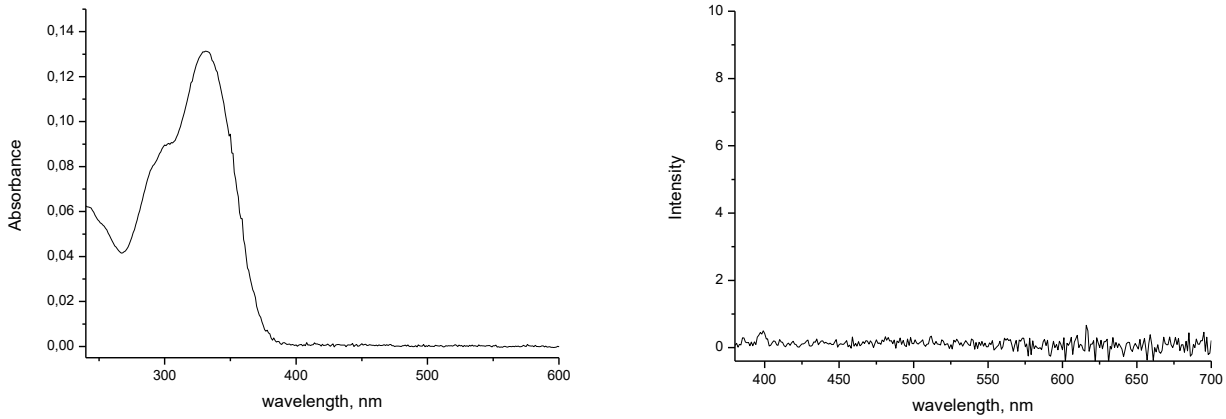

Figure S8 (*a*) Absorption spectrum of ***E*-1** in H_2O, 20°C, $C_{E\text{-}1}$ = 4.6·10^{-6} M; (*b*) fluorescence spectrum of ***E*-1** in H_2O, 20°C, $C_{E\text{-}1}$ = 4.6·10^{-6} M

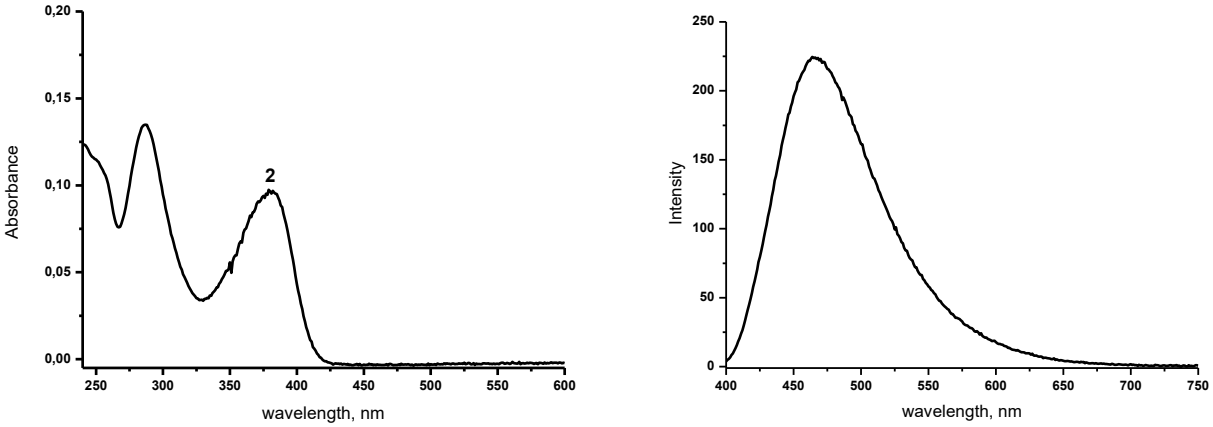

Figure S9 (*a*) Absorption spectrum of **2** in H_2O, 20°C, C_2 = 7.5·10^{-6} M; (*b*) fluorescence spectrum of **2** in H_2O, 20°C, C_2= 7.5·10^{-6} M

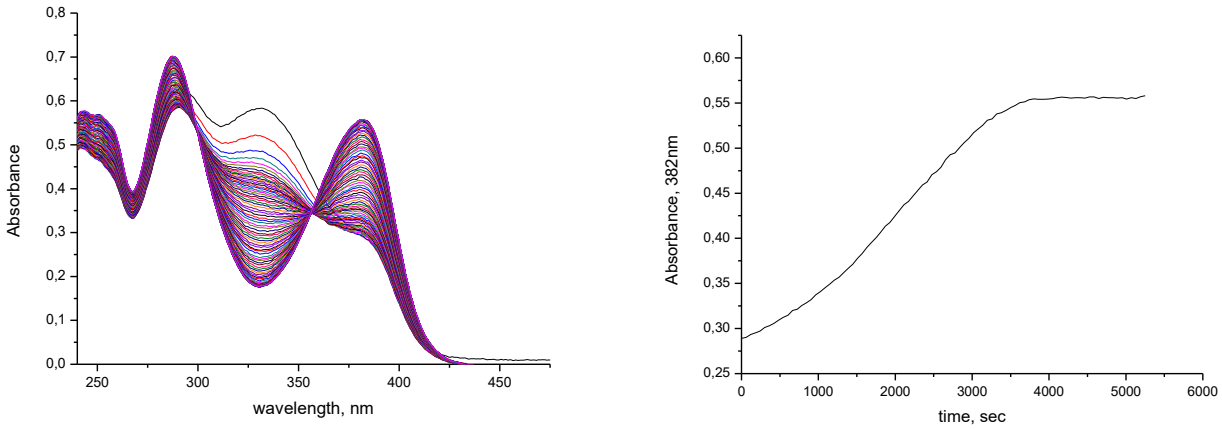

Figure S10 Spectral changes during photolysis of an aqueous solution of styryl **1** and its electrocycle **2** in a 1:1 ratio (left) and kinetics of the formation of a photostationary mixture at 382 nm (right). Mercury lamp with filter 365 nm, $C_{\mathbf{1+2}}$ = 3 10^{-5} M.

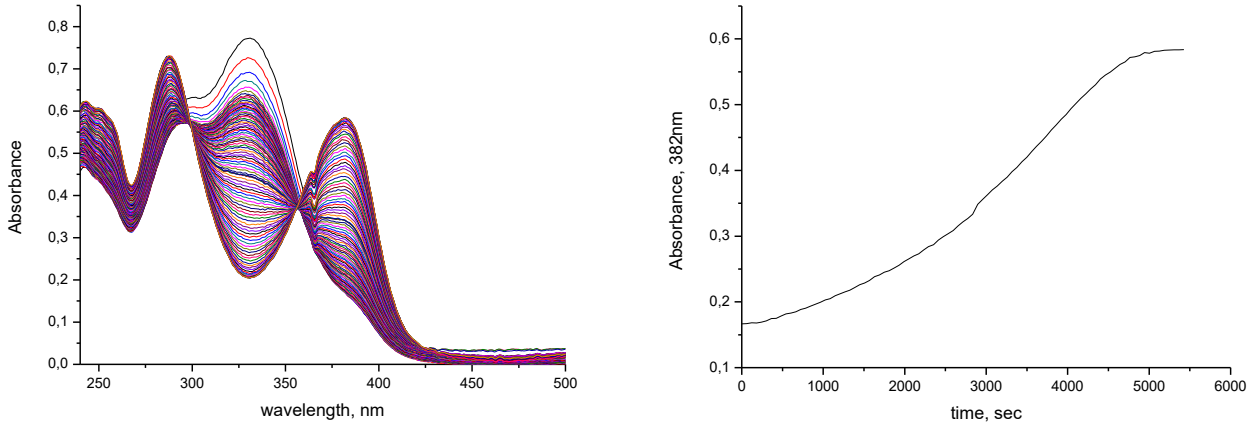

Figure S11 Spectral changes during photolysis of an aqueous solution of styryl **1** and its electrocycle **2** in a 3:1 ratio (left) and kinetics of the formation of a photostationary mixture at 382 nm (right). Mercury lamp with filter 365 nm, $C_{\mathbf{1+2}}$ = 3 10^{-5} M.

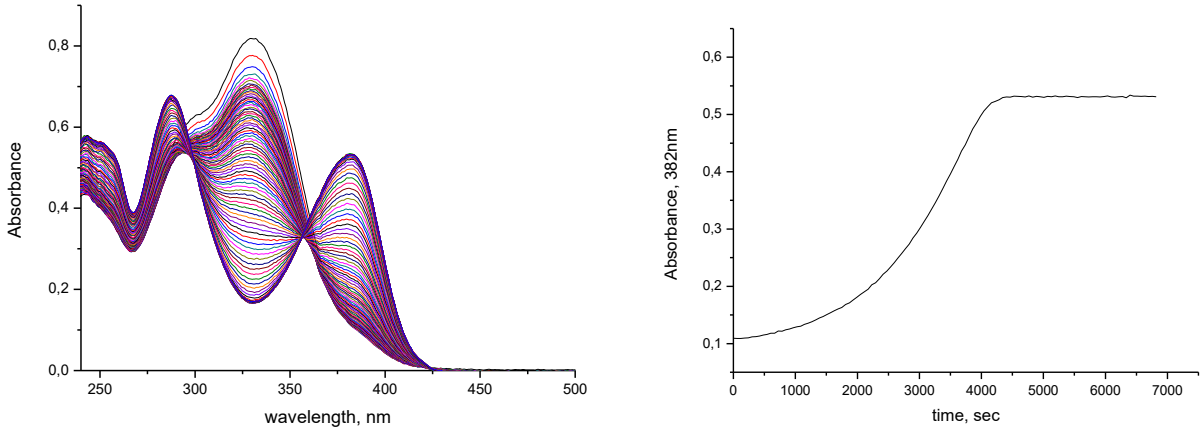

Figure S12 Spectral changes during photolysis of an aqueous solution of styryl **1** and its electrocycle **2** in a 7:1 ratio (left) and kinetics of the formation of a photostationary mixture at 382 nm (right). Mercury lamp with filter 365 nm, $C_{\mathbf{1+2}}$ = 3 10^{-5} M.

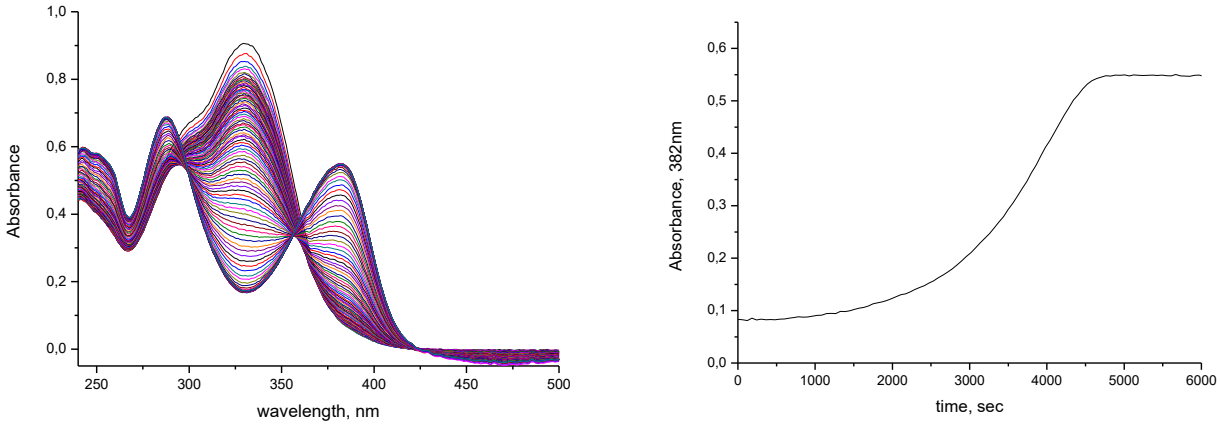

Figure S13 Spectral changes during photolysis of an aqueous solution of styryl **1** and its electrocycle **2** in a 15:1 ratio (left) and kinetics of the formation of a photostationary mixture at 382 nm (right). Mercury lamp with filter 365 nm, $C_{\mathbf{1+2}}$ = 3 10^{-5} M.

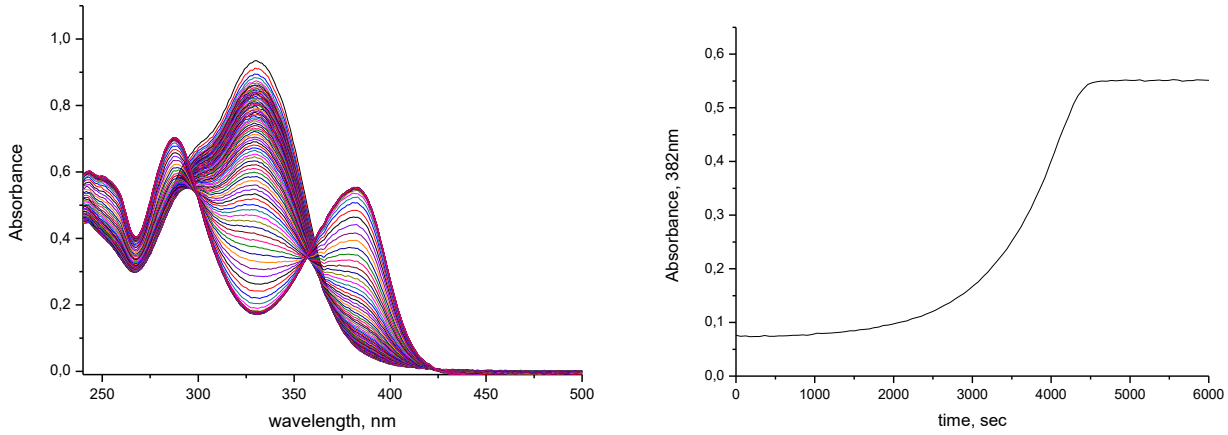

Figure S14 Spectral changes during photolysis of an aqueous solution of styryl **1** and its electrocycle **2** in a 31:1 ratio (left) and kinetics of the formation of a photostationary mixture at 382 nm (right). Mercury lamp with filter 365 nm, $C_{\mathbf{1+2}}$ = 3 10^{-5} M.

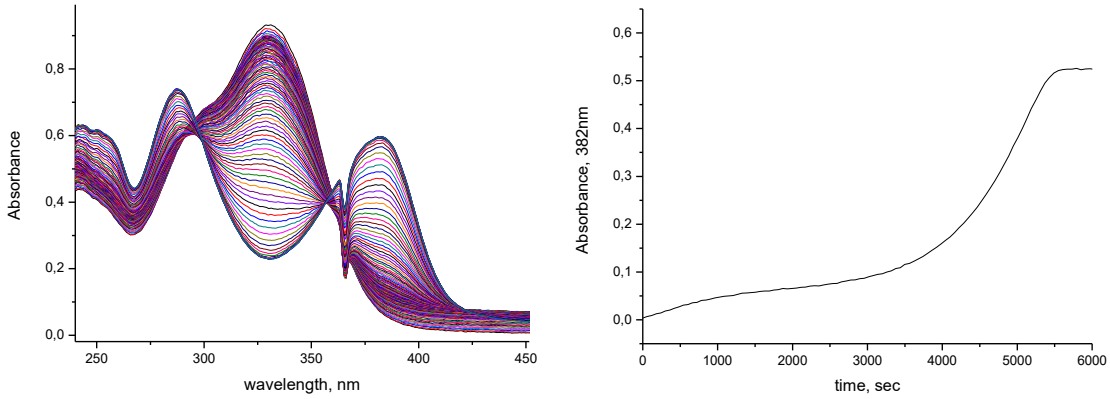

Figure S15 Spectral changes during photolysis of an aqueous solution of styryl **1** and its electrocycle **2** in a 63:1 ratio (left) and kinetics of the formation of a photostationary mixture at 382 nm (right). Mercury lamp with filter 365 nm, $C_{\mathbf{1+2}}$ = 3 10^{-5} M.

References

S1 T. M. Aliyeu, D. V. Berdnikova, O. A. Fedorova, E. N. Gulakova, C. Stremmel and H. Ihmels, *J. Org. Chem.*, 2016, **81**, 9075.

S2 C. L. Renschler and L. A. Harrah, *Anal. Chem.*, 1983, **55**, 798.

S3 A. S. Ovechkin, *PhD Thesis*, 2015.

S4 (*a*) S. Delbaere, J.-C. Micheau and G. Vermeersch, *J. Org. Chem*., 2003, **68**, 8968; (*b*) K. Kaps and P. Rentrop, *Comput. Chem. Eng*., 1984, **8**, 393; (*c*) M. H. Deniel, D. Lavabre and J. C. Micheau, in *Organic Photochromic and Thermodynamic Compounds*, eds. J. C. Crano and R. Guglielmetti, Plenum Press, New York, 1999, vol. 2, pp. 167-209.

S5 G. A. Reynolds and K. H. Drexhage, *Opt. Commun.*, 1975, **13**, 222.